Biochemical and Biophysical Research Communications 451 (2014) 112–118

Contents lists available at ScienceDirect

Biochemical and Biophysical Research Communications

journal homepage: www.elsevier.com/locate/ybbrc

Bufotalin-induced apoptosis in osteoblastoma cells is associated with endoplasmic reticulum stress activation

Yun-Rong Zhu [a,1], Yong Xu [b,1], Jian-Feng Fang [a], Feng Zhou [a], Xiong-Wei Deng [a], Yun-Qing Zhang [a,*]

[a] Department of Orthopedics, The Affiliated Jiangyin Hospital of Medical College of Southeast University, Jiangyin City, Jiangsu 214400, China
[b] Department of Orthopedics, The Second Affiliated Hospital of Soochow University, Suzhou 215000, China

ARTICLE INFO

Article history:
Received 8 July 2014
Available online 25 July 2014

Keywords:
Osteoblastoma
Bufotalin
ER stress
Apoptosis and signaling

ABSTRACT

The search for novel and more efficient chemo-agents against malignant osteoblastoma is important. In this study, we examined the potential anti-osteoblastoma function of bufotalin, and studied the underlying mechanisms. Our results showed that bufotalin induced osteoblastoma cell death and apoptosis in dose- and time-dependent manners. Further, bufotalin induced endoplasmic reticulum (ER) stress activation in osteoblastoma cells, the latter was detected by the induction of C/EBP homologous protein (CHOP), phosphorylation of inositol-requiring enzyme 1 (IRE1) and PKR-like endoplasmic reticulum kinase (PERK), as well as caspase-12 activation. Conversely, the ER stress inhibitor salubrinal, the caspase-12 inhibitor z-ATAD-fmk as well as CHOP depletion by shRNA significantly inhibited bufotalin-induced osteoblastoma cell death and apoptosis. Finally, by using a mice xenograft model, we demonstrated that bufotalin inhibited U2OS osteoblastoma cell growth *in vivo*. In summary, our results suggest that ER stress contributes to bufotalin-induced apoptosis in osteoblastoma cells. Bufotalin might be investigated as a novel anti-osteoblastoma agent.

1. Introduction

Malignant osteoblastoma has one of the worst prognosis among teenagers, and is typically diagnosed at advanced stages [1]. The use of chemotherapy has dramatically improved the overall survival of osteoblastoma patients from 11% in the 1960s, to 70% by the mid-1980s [2]. Since then, survival has not been much improved [3,4]. The malignant osteoblastoma is among the most intrinsically resistant malignancies to almost all chemotherapeutic drugs [5,6]. As such, recent research effects have been focusing on searching for the novel chemo-agents against this disease [5].

Bufotalin is a traditional Chinese medicine prepared from the dried secretion of the auricular and skin glands of Bufo bufo gargarizans Cantor. Recently, bufotalin has drawn attentions from both cancer biologists and oncologists due to its dramatic anti-tumor activities [7–10]. It has been shown that bufotalin inhibits cancer cell growth and induces cancer cell apoptosis *in vivo* and *in vitro* [7–12]. The underlying mechanisms behind the anti-tumor activities of bufotalin are, however, not fully understood. Also, the potential role of bufotalin against osteoblastoma was not studied.

Endoplasmic reticulum (ER) is responsible for the synthesis, modification and delivery of proteins to their proper target sites [13]. ER is also important for intracellular calcium homeostasis [13]. ER could be disrupted when facing various stress conditions causing ER stress [14,15], which activates a signaling network of the unfolded protein response (UPR). Cells respond to ER stress by following mechanisms: (1) to enhance the expression of ER chaperones and folding enzymes; (b) to suppress further misfolded proteins accumulation; and (c) to eliminate misfolded proteins accumulation inside the ER [16]. Although mild ER stress is generally known as a pro-survival and adaptive reaction, prolonged or severe ER stress could promote cell apoptosis [16]. In the current study, we found that ER stress mediates bufotalin-induced apoptosis in osteoblastoma cells.

2. Material and methods

2.1. Chemical and reagents

Salubrinal was purchased from Sigma (St. Louis, MO). The pan-caspase inhibitor z-VAD-fmk and the caspase-12 inhibitor

Abbreviations: ATF6, activating transcription factor 6; CHOP, C/EBP homologous protein; eIF2α, the eukaryotic initiation factor 2α; ER, endoplasmic reticulum; IRE1, inositol-requiring enzyme 1; PERK, double-stranded RNA-activated protein kinase (PKR)-like ER kinase; shRNA, short hairpin RNA; UPR, unfolded protein response.

* Corresponding author. Address: Department of Orthopedics, The Affiliated Jiangyin Hospital of Medical College of Southeast University, No. 163 Shoushan Rd, Jiangyin City, Jiangsu 215600, China.
E-mail address: yunqingzhang@126.com (Y.-Q. Zhang).

[1] Equal contributors.

http://dx.doi.org/10.1016/j.bbrc.2014.07.077
0006-291X/

(z-ATAD-fmk) were purchased from Calbiochem (Darmstadt, Germany). Anti-PKR-like ER kinase (PERK), C/EBP homologous protein (CHOP), inositol-requiring enzyme 1 (IRE-1), tubulin and secondary antibodies were obtained from Santa Cruz Biotechnology (Santa Cruz, CA). Anti-p-IRE1 was obtained from Abcam (Shanghai, China). All other antibodies used in this study were obtained from Cell Signaling Tech (Danvers, MA).

2.2. Cell culture

U2OS, SaOs-2 and MG-63 osteoblastoma cell lines were gifts from Dr. Zhang-ping Gu at Nanjing Medical University [17,18]. Osteoblastoma cells were maintained in DMEM (Sigma, St. Louis, MO), supplemented with a 10% fetal bovine serum (FBS, Sigma) plus penicillin/streptomycin (1:100; Sigma), in a CO_2 incubator at 37 °C. The murine calvaria-derived osteoblastic MC3T3-E1 cells were gift from Dr. Xiaodong Wang at Soochow University [19]. MC3T3-E1 cells were seeded at 1×10^5 cells/ml into 75-cm^2 flasks and maintained in α-MEM supplemented with 10% FBS and 1% penicillin/streptomycin. This basic medium was replenished every 3 days. The cultures were then induced to differentiate by transferring cells into the medium supplemented with L-ascorbic acid (50 μg/ml, Sigma) and β-glycerol phosphate (5 mM, Sigma) [19].

2.3. Cell survival assay (MTT assay)

Cells (1×10^4/well) were seeded in 96-well plates. After treatment, 30 μl of 3-(4,5-dimethylthiazol-2-yl)-2,5-diphenyltetrazolium bromide (MTT) solution (5 mg/ml) were added into each well, and incubated for an additional 4 h. The formazan crystal formed was dissolved with 100 μl of DMSO. Absorbance was measured at 490 nm by a microplate reader (Bio-Rad, Nanjing, China). Absorbance of cells with no treatment (control group) was regarded as 100% cell survival.

2.4. Trypan blue staining of "dead" cells

After treatment, dead cells were stained by trypan blue, and the percentage (%) was calculated by the number of the trypan blue stained cells dividing by the total cell number, which was automatically recorded by a handheld automated cell counter (Merck Millipore, Shanghai, China).

2.5. Clonogenicity assay

Cells (5×10^4) were suspended in 1 ml of DMEM containing 1% agar (Sigma, St. Louis, MO), 10% FBS and with indicated treatment. The cell suspension was then added on top of a pre-solidified 1% agar in a 100 mm culture dish. The medium was replaced every 2 days. After 10-day of incubation, colonies were photographed. Colonies with diameter larger than 50 μm were recorded and counted manually.

2.6. Western blotting and data quantification

After treatments, the cells were washed with ice-cold phosphate buffered saline (PBS) and then lysed using lysis buffer (pH, 7.4) containing 50 mM Tris [pH 8.0], 250 mM NaCl, 1% NP-40, 0.1% sodium dodecyl sulfate, 5 mM EDTA, 2 mM Na_3VO_4, 10 mM $Na_2P_2O_7$, 10 mM NaF and 1 mM phenylmethylsulfonyl fluoride [17]. The lysates were collected and centrifuged. The protein concentration was determined by using a Bio-Rad Bradford protein assay kit (Bio-Rad, Shanghai, China). The extracted protein sample was boiled for 5 min in 5-time loading buffer. Samples were separated by 10% SDS–polyacrylamide gel, and electro-transferred onto a polyvinylidene fluoride (PVDF) membrane (Millipore, USA). Afterwards, the membrane was blocked with blocking buffer (10% (w/v) milk in PBS Tween-20 (PBST), incubated overnight at 4 °C with the indicated primary antibody, and then incubated with HRP-conjugated second antibody at room temperature for 1–2 h. The detection was performed by ECL Supersignal West Pico Chemiluminescent Substrate according to the manufacturer's instruction. The intensity of indicated band was quantified by densitometry using ImageJ software, and was normalized to the loading control. Quantification value was expressed as the fold change vs. the band labeled with "1.00". ImageJ was downloaded from NIH website [20].

2.7. Annexin V-FITC/propidium iodine (PI) double staining assay

Annexin V-FITC/PI double staining assay was performed according to the manufacturer's instructions. Briefly, cells (about 6×10^5/well) were harvested immediately after treatment, and then incubated in 100 μl of labeling solution, which contained 5 μl of Annexin V-FITC, 5 μl of PI, 10 μl of 10-time binding buffer and 75 μl of H_2O (R&D Systems, Minneapolis, MN), in darkness at room temperature for 15 min. After that, 400 μl of 1-time binding buffer was added to stop the staining reaction. The stained cells were detected in FL1 and FL3 fluorescence channels using FACSort flow cytometry system (Becton Dickinson, Shanghai, China). The percentage of Annexin V was detected as an indicator of apoptosis rate.

2.8. Cell cycle analysis

Cell cycle distribution of MG-63 cells was detected by flow cytometry. Briefly, after treatment, MG-63 cells (about 6×10^5/well) were collected and fixed in 70% ethanol at 4 °C overnight. Before analysis, cells were centrifuged at 2500 rpm for 3 min to remove the ethanol. Then, cells were suspended in 500 μl PBS containing 0.02 mg/ml PI and 0.1 mg/ml Ribonuclease A (RNase A) in darkness at 37 °C for 30 min. Fluorescence emitted from PI-DNA complexes was measured by Becton Dickinson (Shanghai, China). Cell distribution in different phases of cell cycle was then analyzed through Becton Dickinson software.

2.9. Caspase-12 activity assay

After treatment, cytosolic proteins from approximately 2–3×10^6 cells were extracted in hypotonic cell lysis buffer (25 mm HEPES, pH 7.5, 5 mM $MgCl_2$, 5 mM EDTA, 5 mM dithiothreitol, 0.05% phenylmethylsulfonyl fluoride). 20 μg of cytosolic extracts were added to caspase assay buffer (312.5 mM HEPES, pH 7.5, 31.25% sucrose, 0.3125% CHAPS) with ATAD-7-amido-4-(trifluoromethyl) coumarin (AFC) (15 μg/ml) (Calbiochem, Darmstadt, Germany) as the substrate. After incubation at 37 °C for 1 h, the amount of AFC liberated from ATAD-AFC was measured using a spectrofluorometer (Thermo-Labsystems, Helsinki, Finland) with excitation of 380 nm and emission wavelength of 460 nm.

2.10. CHOP shRNA-knockdown through lentiviral infection

Two different human CHOP shRNAs (targeting non-overlapping human *CHOP* cDNA sequence) and one scramble shRNA containing lentiviral particles were designed and synthesised by Kaiji Biotech (Shanghai, China). Osteoblastoma cells were seeded in a six-well plate in the growth medium. The lentiviral particles (15 μl/ml medium) were added to the cells. After 12 h, the medium was replaced by fresh growth medium, and cells were further cultured for additional 48 h. The expression of target protein (CHOP) and the equal loading (tubulin) in the infected cells was detected by Western blotting.

2.11. Mice U2OS xenograft

CB.17 severe combined immuno-deficient (SCID) male mice (4–6 weeks old) were maintained at the animal facility of Southeast University and handled according to institutional regulations, under sterile conditions in cage micro isolators. Mice was injected subcutaneously (s.c.) into the right flank with 2×10^6 U2OS cells in 0.1 ml DMEM/10% FBS. When the right flank xenografts were established at about 500 mm^3, the animals (10 mice per group) were administrated i.p. twice daily (b.i.d) with 0.5–1 mg/kg (in saline) of bufotalin for 7 consecutive days. The xenografted tumor diameter was measured every 7 days using calipers. Tumor volumes (V) were calculated using the following formula: $V = A \times B^2/2$ (A = largest diameter; B = smallest diameter). Mice body weight was also recorded every week. We were unable to establish a MG-63 xenograft model in this study. All animals were maintained in accordance with the guidelines of the NIH (Guide for the Care and Use of Laboratory Animals). The protocol is approved by Animal Care and Use Committee of all authors' institutions.

2.12. Statistics

The data presented were mean ± standard deviation (SD). Statistical differences were analyzed by one-way ANOVA followed by multiple comparisons performed with post hoc Bonferroni test (SPSS version 16). Values of $p < 0.05$ were considered statistically significant.

3. Results

3.1. The cytotoxic effect of bufotalin in osteoblastoma cells

We first tested the potential effect of bufotalin in cultured osteoblastoma cells. The MTT cell viability assay results in Fig. 1A demonstrated that bufotalin dose-dependently inhibited MG-63 osteoblastoma cell survival. Same doses of bufotalin only induced a minor inhibition on osteoblastic MC3T3-E1 cell viability (Fig. 1A), suggesting its unique cytotoxic effect in cancer cells. Results also showed that it took at least 48 h for bufotalin (1 μM) to inhibit MG-63 cell viability (Fig. 1B). Further, bufotalin treatment increased the number of trypan blue positive ("dead") MG-63 cells (Fig. 1C). The cytotoxicity of bufotalin against osteoblastoma cells was further shown by the "clonogenicity" assay, as the number of survival colonies was significantly decreased after bufotalin treatment (Fig. 1D). Results in Fig. 1E showed that bufotalin inhibited viability of two other osteoblastoma cell lines: U2OS and SaOs-2. Together, these results show the cytotoxic effect of bufotalin in cultured osteoblastoma cells.

3.2. Bufotalin-induced osteoblastoma cell apoptosis is associated with caspase-12 activation

Next, we tested whether cell apoptosis contributed to bufotalin cytotoxicity in osteoblastoma cells. Results in Fig. 2A and B demonstrated that bufotalin dose-dependently increased the percentage of Annexin V positive cells (apoptotic cells) and caspase-12 activity in MG-63 cells, which were inhibited by pre-treatment with pan-caspase inhibitor (z-VAD-fmk, zVAD) and caspase-12 inhibitor (z-ATAD-fmk, ATAD). Western blot results further confirmed caspase-12 activation by bufotalin in MG-63 cells (Fig. 2C). Above caspase inhibitors zVAD and ATAD dramatically inhibited bufotalin (1 μM)-induced MG-63 cell viability decrease (Fig. 2D) and cell death (Fig. 2E). Together, these results demonstrate that bufotalin induces caspase-12-dependent cell apoptosis in osteoblastoma cells. Annexin V FACS results in Fig. 2F showed apoptosis activation by bufotalin in U2OS and SaOs-2 osteoblastoma cell lines. Previous studies have shown that the inhibitory role of bufotalin on certain cancer cells was associated with cell cycle arrest [8]. Next we tested its effect on MG-63 cell cycle progression. As shown in

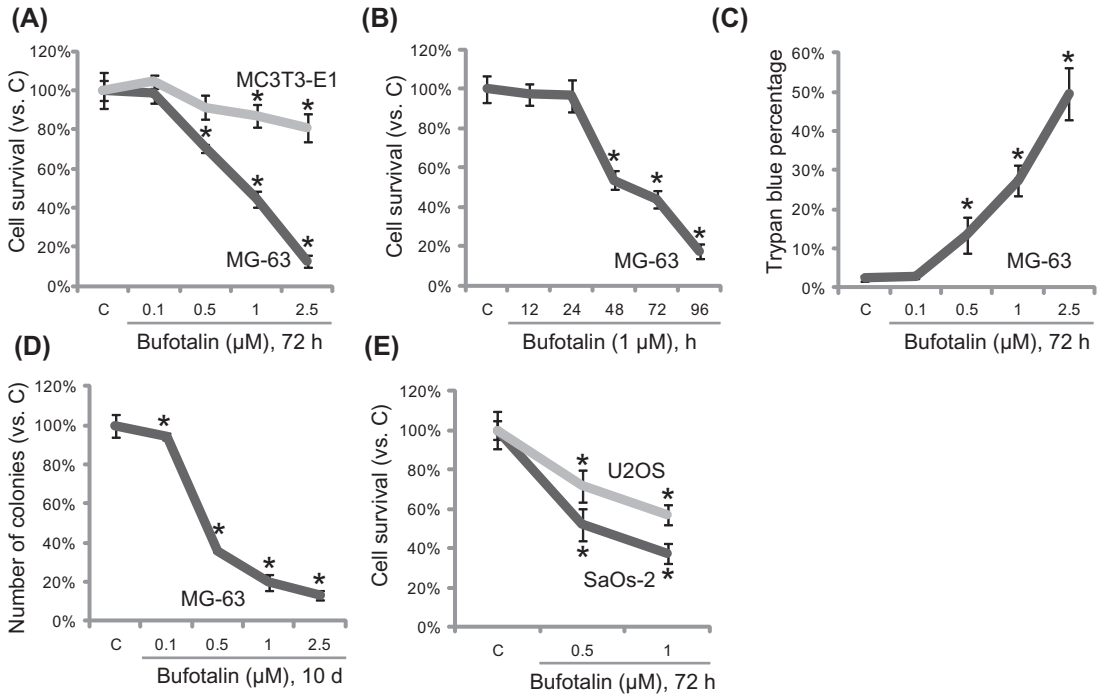

Fig. 1. The cytotoxic effect of bufotalin in osteoblastoma cells. The cell viability of MG-63 osteoblastoma cells or MC3T3-E1 osteoblastic cells with indicated bufotalin treatment was analyzed by MTT assay (A and B). MG-63 cells were treated with indicated concentration of bufotalin, trypan blue staining (C) and "clonogenicity" (D) were performed to test cell death. The cell viability of U2OS and SaOs-2 cells with indicated bufotalin treatment was also shown (E). "C" stands for untreated control. $n = 5$ for each assay. The data in this figure were representatives of three different experiments. The values were expressed as the means ± SD. $^*p < 0.05$ vs. group "C".

Fig. 2G and H, bufotalin (1 μM) showed no significant effect on MG-63 cell cycle progression. The cell cycle distribution in bufotalin-treated MG-63 cells was almost the same as that of untreated control cells. We also tested dose–response (up to 2.5 μM) and time-course response (up to 72 h) of bufotalin on cell cycle progression, and observed similar results (Data not shown). Meanwhile, the cell cycle distribution of U2OS and SaOs-2 cells was also not affected by bufotalin (Data not shown).

3.3. ER stress inhibitor salubrinal suppresses bufotalin-induced cytotoxicity in osteoblastoma cells

Caspase-12 is an important mediator of ER stress-mediated apoptosis [21], our results have shown that bufotalin-induced osteoblastoma cell apoptosis was associated with caspase-12 activation (Fig. 2). We thus tested the effect of bufotalin on ER stress activation, which was detected by the induction of CHOP as well as phosphorylation of PERK and IRE1 [13]. As demonstrated, bufotalin dose-dependently induced CHOP expression as well as PERK and IRE1 phosphorylation in MG-63 cells (Fig. 3A). Significantly, ER stress inhibitor salubrinal (Sal) [22] dramatically inhibited bufotalin-induced MG-63 cell viability decrease and cell death (Fig. 3B and C). Cell apoptosis by bufotalin was also inhibited by Sal in MG-63 cells (Fig. 3D). Further, bufotalin-induced cytotoxicity in U2OS and SaOs-2 cells were also inhibited by Sal pre-treatment (Fig. 3E and F). Together, these results show that bufotalin-induced osteoblastoma cell apoptosis is associated with ER stress activation.

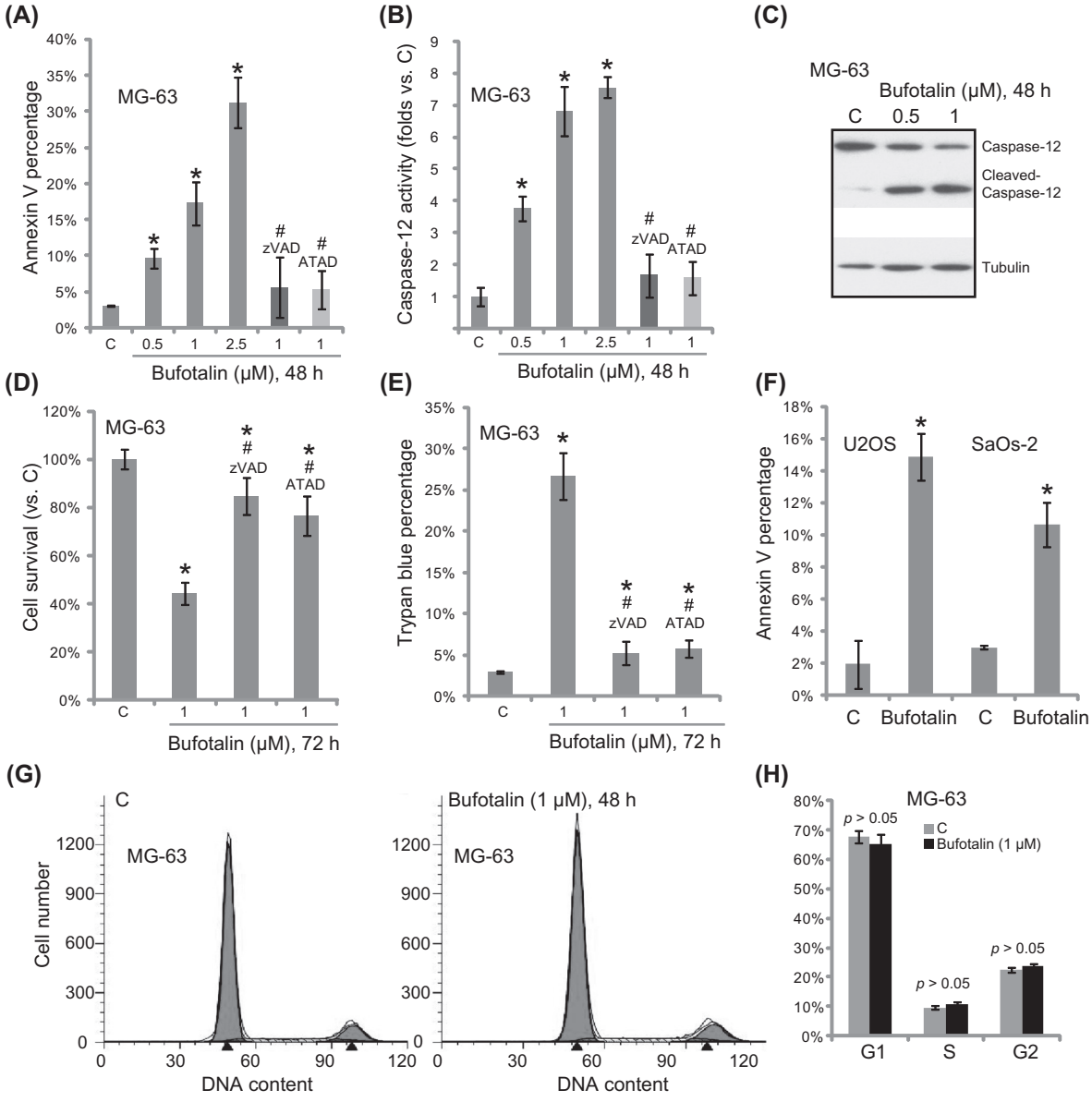

Fig. 2. Bufotalin-induced osteoblastoma cell apoptosis is associated with caspase-12 activation. MG-63 cells were treated with indicated concentration of bufotalin, or with z-VAD-fmk (zVAD, 25 μM) or z-ATAD-fmk (ATAD, 25 μM) for 48 h, Annexin V FACS assay (A) and caspase-12 activity assay (B) were performed. The expression of caspase-12 and tubulin (equal loading) was tested by Western blotting (C). MG-63 cells were pretreated with z-VAD-fmk (zVAD, 25 μM) or z-ATAD-fmk (ATAD, 25 μM) for 1 h, followed by bufotalin (1 μM) stimulation, cells were further cultured for 72 h, MTT assay (D) and trypan blue staining (E) were utilized to test cell viability and cell death, respectively. Apoptosis in bufotalin (1 μM, 48 h)-treated U2OS and SaOs-2 cells was analyzed by Annexin V FACS assay (F). Cell cycle distribution in MG-63 cells treated with or without bufotalin (1 μM, 48 h) was examined by FACS assay (G and H). "C" stands for untreated control. $n = 5$ for each assay. The data in this figure were representatives of three different experiments. The values were expressed as the means ± SD. $^{*}p < 0.05$ vs. group "C". $^{\#}p < 0.05$ vs. bufotalin (1 μM) only group.

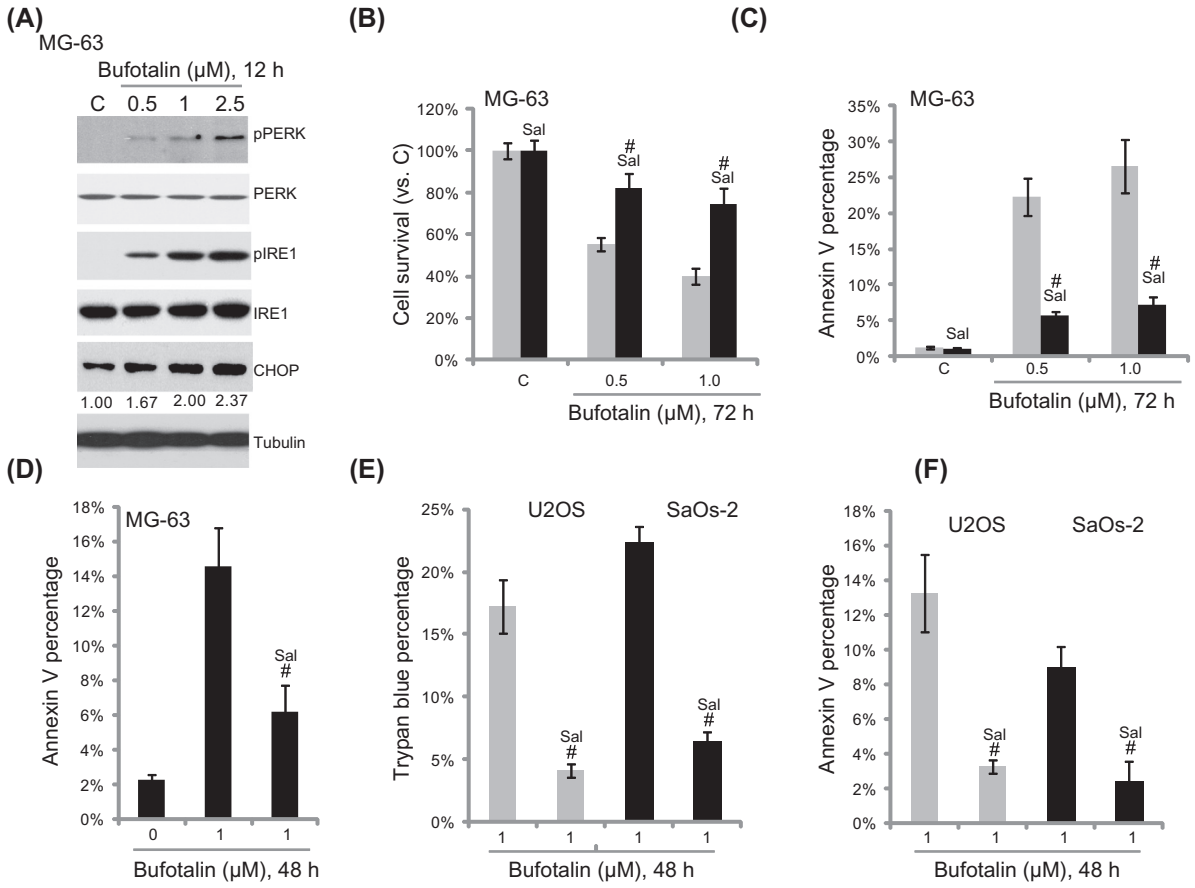

Fig. 3. ER stress inhibitor salubrinal suppresses bufotalin-induced cytotoxicity in osteoblastoma cells. MG-63 cells were treated with indicated concentration of bufotalin for 12 h, expression of indicated proteins was examined by Western blotting using specific antibodies (A). MG-63/U2OS/SaOs-2 cells were pretreated with ER stress inhibitor salubrinal (Sal, 25 μM) for 1 h, followed by indicated bufotalin exposure, cell viability, cell death and apoptosis were tested by MTT assay (B), trypan blue staining (C and E) and Annexin V FACS assay (D and F), respectively. "C" stands for untreated control. The data in this figure were representatives of three different experiments. The values were expressed as the means ± SD. $^{\#}p < 0.05$ vs. bufotalin only group.

3.4. CHOP silencing inhibits bufotalin-induced osteoblastoma cell apoptosis

CHOP is an important regulator of ER stress-induced apoptosis [23,24]. Above results have shown that bufotalin increased CHOP expression in osteoblastoma cells. Next, we explored the role of CHOP in bufotalin-induced apoptosis. By using the shRNA strategy, we efficiently knockdown CHOP expression in MG-63 cells. Note that we utilized two targeted shRNAs against two non-overlapping sequence of human *CHOP* cDNA. Both shRNAs dramatically down-regulated CHOP expression in MG-63 cells (Fig. 4A). bufotalin-induced MG-63 cell death (tested by trypan blue staining) and apoptosis (tested by Annexin V FACS) were dramatically inhibited by CHOP shRNA-knockdown (Fig. 4B). Further, in two other osteoblastoma cell lines (U2OS and SaOs-2), CHOP depletion similarly inhibited cell apoptosis induction by bufotalin (Fig. 4C and D). These results suggest that CHOP is important for bufotalin-induced apoptosis in osteoblastoma cells.

3.5. Bufotalin inhibits U2OS cell growth in vivo

Finally, by using a mice U2OS OS xenograft model, we tested the anti-osteoblastoma activity of bufotalin *in vivo*. As shown in Fig. 4E, the mice that received bufotalin (0.5–1 mg/kg, i.p. twice per day, for 7 days) showed a significantly reduced tumor growth as compared to mice that received vehicle control (PBS). The mice body weight was not significantly affected by bufotalin administration, indicating the relative safety of this bufotalin treatment regimen (Fig. 4F). Note that the concentration and treatment duration of bufotalin were chosen based on previous publications and pre-experimental results. These results confirm that bufotalin inhibits U2OS osteoblastoma cell growth *in vivo*.

4. Discussions

When cells facing ER stresses, the corresponding UPR is primarily an adaptive and pro-survival response, aiming to restore ER homeostasis as well as protecting the cells [16]. ER stress activates three ER stress sensors including PERK, IRE1 and activating transcription factor 6 (ATF6) [13]. IRE1 could recruit TNF receptor-associated factor 2 (TRAF2) and apoptosis signal-regulating kinase 1 (ASK1) to activate p38 and JNK signaling pathways [13]. Activated PERK mediates phosphorylation of the translation initiation factor eukaryotic translation initiation factor 2 (eIF2α) [13]. ATF6 will translocate to Golgi where it is subsequently cleaved to become an active transcription factor [13]. However, if the stress is severe, prolonged or unsolved, and the adaptive response fails, UPR receptors could then initiate a pro-apoptotic response to promote cell apoptosis [16]. In the current study, we found that the ER stress inhibitor Sal significantly alleviated bufotalin-mediated apoptosis and cytotoxicity in osteoblastoma cells, suggesting an important role of ER stress in bufotalin-mediated cell apoptosis.

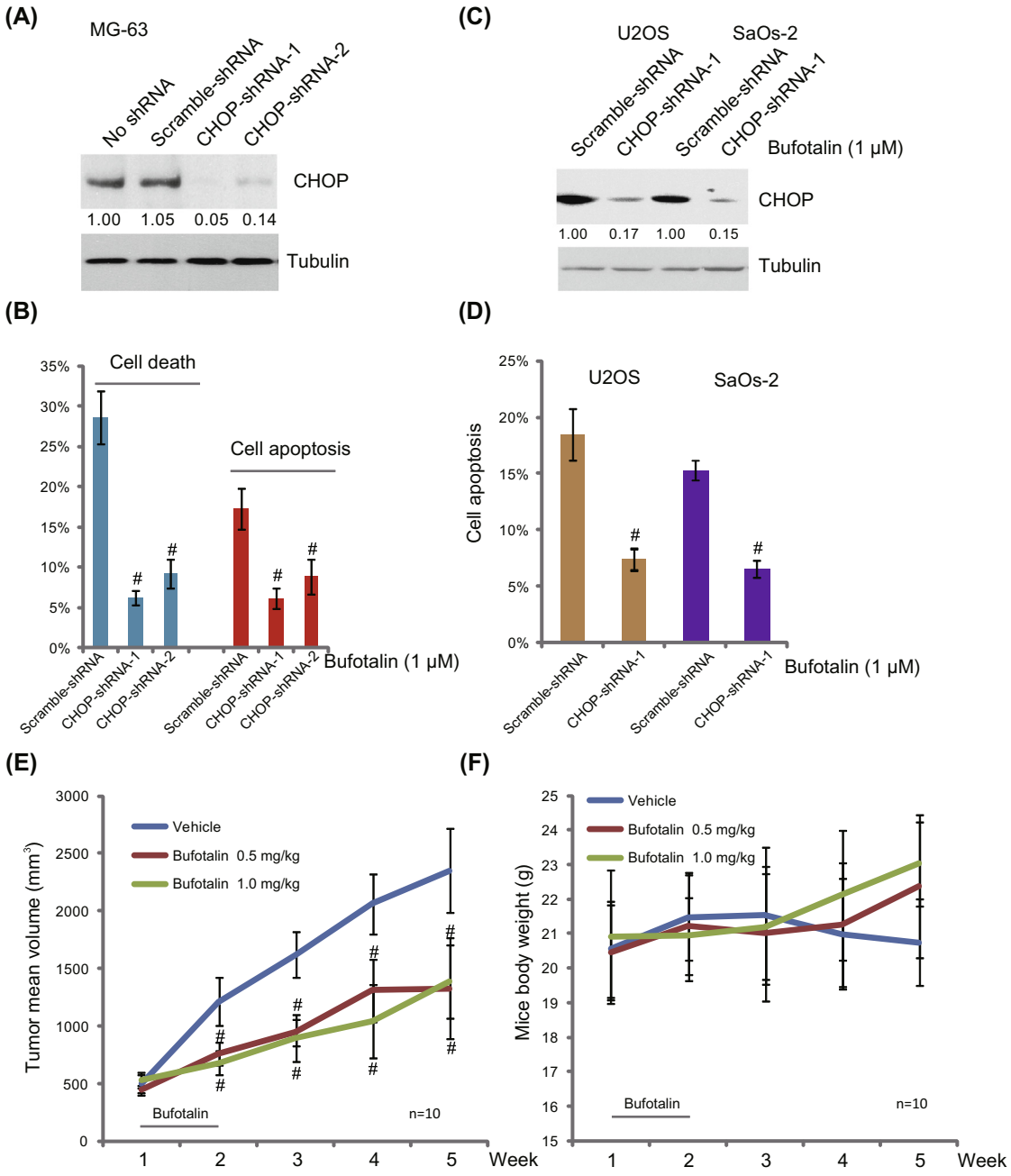

Fig. 4. CHOP silencing inhibits bufotalin-induced osteoblastoma cell apoptosis. CHOP and tubulin expression in control MG-63 cells, or infected with scramble-shRNA, CHOP-1-shRNA-1 or CHOP-shRNA-2 (15 μl/ml each, 48 h) was tested by Western blotting (A). Above cells were treated with bufotalin (1 μM), cell death (tested by trypan blue staining, 72 h) and apoptosis (tested by Annexin V assay, 48 h) were also shown (B). U2OS/SaOs-2 cells were infected with scramble-shRNA or CHOP-1-shRNA-1 (15 μl/ml each, 48 h), cells were further treated with bufotalin (1 μM) for 72 h, CHOP expression was tested by Western blotting (C), and cell death was tested by the Trypan blue staining assay (D). The U2OS cell xenografted mice (10 mice per group) were treated with twice daily (b.i.d) with bufotalin (0.5/1 mg/kg, i.p., 7 days) or vehicle (PBS), tumor size was measured every 7 days (E). Mice body weight was also recorded every week (F). The data in this figure were representatives of three different experiments. The values were expressed as the means ± SD. $^{\#}p < 0.05$ vs. scramble shRNA group (B and D). $^{\#}p < 0.05$ vs. vehicle control group (E).

Although ER stress-induced apoptotic pathway is still not fully characterized, two specific hallmarks of the process have been identified, including upregulation of the pro-apoptotic transcription factor CHOP [24,25] and activation of the ER-localized caspase: caspase-12 [21]. The pro-apoptotic transcription factor CHOP can be up-regulated by IRE1, ATF6 and PERK, and can mediate transcription of the pro-apoptotic BH3-only protein Bim [26]. We found that bufotalin induced CHOP expression in osteoblastoma cells. While CHOP depletion by shRNAs largely inhibited bufotalin-induced osteoblastoma cell death and apoptosis. Thus, CHOP is an important mediator of ER stress-induced apoptosis by bufotalin in osteoblastoma cells.

Activated IRE1 provides a platform for the recruitment of caspase-12 at the ER membrane and results in its proteolytic processing activation, which eventually promotes cell apoptosis [21,27]. However, studies have also shown that caspase-12 deficient mouse embryonic fibroblasts (MEFs) display no resistance against ER stress inducing agents [28,29]. Here in this study, we

observed caspase-12 activation by bufotalin in osteoblastoma cells. Our data suggested that caspase-12 might be required for ER stress-induced apoptosis by bufotalin, based on the fact that caspase-12 inhibitor significantly alleviated bufotalin-induced apoptosis and cytotoxicity in osteoblastoma cells.

In summary, we conclude that ER stress contributes to bufotalin-induced apoptosis in osteoblastoma cells. Our *in vitro* and *in vivo* results suggest that bufotalin might be investigated as a novel anti-osteoblastoma agent.

Conflict of interest

The authors declare that they have no conflict of interest.

Acknowledgment

This work is supported by the National Science Foundation of China.

References

[1] S.J. Ham, H. Schraffordt Koops, W.T. van der Graaf, J.R. van Horn, L. Postma, H.J. Hoekstra, Historical, current and future aspects of osteosarcoma treatment, Eur. J. Surg. Oncol. 24 (1998) 584–600.
[2] A.J. Chou, R. Gorlick, Chemotherapy resistance in osteosarcoma: current challenges and future directions, Expert Rev. Anticancer Ther. 6 (2006) 1075–1085.
[3] S. Berberoglu, A. Oguz, E. Aribal, O. Ataoglu, Osteoblastoma response to radiotherapy and chemotherapy, Med. Pediatr. Oncol. 28 (1997) 305–309.
[4] B. Camitta, R. Wells, A. Segura, K.K. Unni, K. Murray, D. Dunn, Osteoblastoma response to chemotherapy, Cancer 68 (1991) 999–1003.
[5] S.J. Zardawi, S.A. O'Toole, R.L. Sutherland, E.A. Musgrove, Dysregulation of hedgehog, Wnt and notch signalling pathways in breast cancer, Histol. Histopathol. 24 (2009) 385–398.
[6] L. Gorelik, R.A. Flavell, Transforming growth factor-beta in T-cell biology, Nat. Rev. Immunol. 2 (2002) 46–53.
[7] C.L. Su, T.Y. Lin, C.N. Lin, S.J. Won, Involvement of caspases and apoptosis-inducing factor in bufotalin-induced apoptosis of Hep 3B cells, J. Agric. Food Chem. 57 (2009) 55–61.
[8] D.M. Zhang, J.S. Liu, M.K. Tang, A. Yiu, H.H. Cao, L. Jiang, J.Y. Chan, H.Y. Tian, K.P. Fung, W.C. Ye, Bufotalin from Venenum Bufonis inhibits growth of multidrug resistant HepG2 cells through G2/M cell cycle arrest and apoptosis, Eur. J. Pharmacol. 692 (2012) 19–28.
[9] P. Waiwut, A. Inujima, H. Inoue, I. Saiki, H. Sakurai, Bufotalin sensitizes death receptor-induced apoptosis via Bid- and STAT1-dependent pathways, Int. J. Oncol. 40 (2012) 203–208.
[10] T. Nogawa, Y. Kamano, A. Yamashita, G.R. Pettit, Isolation and structure of five new cancer cell growth inhibitory bufadienolides from the Chinese traditional drug Ch'an Su, J. Nat. Prod. 64 (2001) 1148–1152.
[11] C.H. Yu, S.F. Kan, H.F. Pu, E. Jea Chien, P.S. Wang, Apoptotic signaling in bufalin- and cinobufagin-treated androgen-dependent and -independent human prostate cancer cells, Cancer Sci. 99 (2008) 2467–2476.
[12] K.Q. Han, G. Huang, W. Gu, Y.H. Su, X.Q. Huang, C.Q. Ling, Anti-tumor activities and apoptosis-regulated mechanisms of bufalin on the orthotopic transplantation tumor model of human hepatocellular carcinoma in nude mice, World J. Gastroenterol. 13 (2007) 3374–3379.
[13] T. Verfaillie, A.D. Garg, P. Agostinis, Targeting ER stress induced apoptosis and inflammation in cancer, Cancer Lett. 332 (2013) 249–264.
[14] S.J. Healy, A.M. Gorman, P. Mousavi-Shafaei, S. Gupta, A. Samali, Targeting the endoplasmic reticulum-stress response as an anticancer strategy, Eur. J. Pharmacol. 625 (2009) 234–246.
[15] D. Wlodkowic, J. Skommer, D. McGuinness, C. Hillier, Z. Darzynkiewicz, ER-golgi network – a future target for anti-cancer therapy, Leuk. Res. 33 (2009) 1440–1447.
[16] C. Hetz, The unfolded protein response: controlling cell fate decisions under ER stress and beyond, Nat. Rev. Mol. Cell Biol. 13 (2012) 89–102.
[17] C. Yao, S. Wu, D. Li, H. Ding, Z. Wang, Y. Yang, S. Yan, Z. Gu, Co-administration phenoxodiol with doxorubicin synergistically inhibit the activity of sphingosine kinase-1 (SphK1), a potential oncogene of osteosarcoma, to suppress osteosarcoma cell growth both in vivo and in vitro, Mol. Oncol. 6 (2012) 392–404.
[18] C. Yao, J.J. Wei, Z.Y. Wang, H.M. Ding, D. Li, S.C. Yan, Y.J. Yang, Z.P. Gu, Perifosine induces cell apoptosis in human osteosarcoma cells: new implication for osteosarcoma therapy?, Cell Biochem Biophys. 65 (2013) 217–227.
[19] Y.F. Zhen, G.D. Wang, L.Q. Zhu, S.P. Tan, F.Y. Zhang, X.Z. Zhou, X.D. Wang, P53 dependent mitochondrial permeability transition pore opening is required for dexamethasone-induced death of osteoblasts, J. Cell Physiol. (2014).
[20] L.Q. Zhu, Y.F. Zhen, Y. Zhang, Z.X. Guo, J. Dai, X.D. Wang, Salinomycin activates AMP-activated protein kinase-dependent autophagy in cultured osteoblastoma cells: a negative regulator against cell apoptosis, PLoS One 8 (2013) e84175.
[21] T. Nakagawa, H. Zhu, N. Morishima, E. Li, J. Xu, B.A. Yankner, J. Yuan, Caspase-12 mediates endoplasmic-reticulum-specific apoptosis and cytotoxicity by amyloid-beta, Nature 403 (2000) 98–103.
[22] M. Boyce, K.F. Bryant, C. Jousse, K. Long, H.P. Harding, D. Scheuner, R.J. Kaufman, D. Ma, D.M. Coen, D. Ron, J. Yuan, A selective inhibitor of eIF2alpha dephosphorylation protects cells from ER stress, Science 307 (2005) 935–939.
[23] S. Oyadomari, M. Mori, Roles of CHOP/GADD153 in endoplasmic reticulum stress, Cell Death Differ. 11 (2004) 381–389.
[24] H. Yamaguchi, H.G. Wang, CHOP is involved in endoplasmic reticulum stress-induced apoptosis by enhancing DR5 expression in human carcinoma cells, J. Biol. Chem. 279 (2004) 45495–45502.
[25] H. Zinszner, M. Kuroda, X. Wang, N. Batchvarova, R.T. Lightfoot, H. Remotti, J.L. Stevens, D. Ron, CHOP is implicated in programmed cell death in response to impaired function of the endoplasmic reticulum, Genes Dev. 12 (1998) 982–995.
[26] H. Puthalakath, L.A. O'Reilly, P. Gunn, L. Lee, P.N. Kelly, N.D. Huntington, P.D. Hughes, E.M. Michalak, J. McKimm-Breschkin, N. Motoyama, T. Gotoh, S. Akira, P. Bouillet, A. Strasser, ER stress triggers apoptosis by activating BH3-only protein Bim, Cell 129 (2007) 1337–1349.
[27] J.A. Martinez, Z. Zhang, S.I. Svetlov, R.L. Hayes, K.K. Wang, S.F. Larner, Calpain and caspase processing of caspase-12 contribute to the ER stress-induced cell death pathway in differentiated PC12 cells, Apoptosis 15 (2010) 1480–1493.
[28] H. Shiraishi, H. Okamoto, A. Yoshimura, H. Yoshida, ER stress-induced apoptosis and caspase-12 activation occurs downstream of mitochondrial apoptosis involving Apaf-1, J. Cell Sci. 119 (2006) 3958–3966.
[29] T. Yoneda, K. Imaizumi, K. Oono, D. Yui, F. Gomi, T. Katayama, M. Tohyama, Activation of caspase-12, an endoplastic reticulum (ER) resident caspase, through tumor necrosis factor receptor-associated factor 2-dependent mechanism in response to the ER stress, J. Biol. Chem. 276 (2001) 13935–13940.